Hindawi
Shock and Vibration
Volume 2019, Article ID 6294814, 11 pages
https://doi.org/10.1155/2019/6294814

Research Article

Nonlinear Parametric Vibration and Chaotic Behaviors of an Axially Accelerating Moving Membrane

Mingyue Shao[1,2] **Jimei Wu**[1,2] **Yan Wang**[3] **and Qiumin Wu**[2]

[1]*School of Mechanical and Precision Instrument Engineering, Xi'an University of Technology, Xi'an 710048, China*
[2]*School of Printing, Packaging and Digital Media Engineering, Xi'an University of Technology, Xi'an 710048, China*
[3]*School of Civil Engineering and Architecture, Xi'an University of Technology, Xi'an 710048, China*

Correspondence should be addressed to Jimei Wu; wujimei1@163.com

Received 5 September 2018; Revised 17 January 2019; Accepted 18 February 2019; Published 11 March 2019

Academic Editor: Francesco Pellicano

Nonlinear vibration characteristics of a moving membrane with variable velocity have been examined. The velocity is presumed as harmonic change that takes place over uniform average speed, and the nonlinear vibration equation of the axially moving membrane is inferred according to the D'Alembert principle and the von Kármán nonlinear thin plate theory. The Galerkin method is employed for discretizing the vibration partial differential equations. However, the solutions concerning to differential equations are determined through the 4^{th} order Runge–Kutta technique. The results of mean velocity, velocity variation amplitude, and aspect ratio on nonlinear vibration of moving membranes are emphasized. The phase-plane diagrams, time histories, bifurcation graphs, and Poincaré maps are obtained; besides that, the stability regions and chaotic regions of membranes are also obtained. This paper gives a theoretical foundation for enhancing the dynamic behavior and stability of moving membranes.

1. Introduction

Membrane materials are extensively used in the packaging and printing industry; together with this, it is also used in mechanical instruments, aerospace, biomedical science, and some other fields. In engineering activities, the membrane is not strictly possessing a uniform motion; for instance, the disturbance appears during the rotation of a guide roller in the printing process, it would result in the change in membrane velocity, and the vibration characteristics of the membrane would become highly complex; in certain cases, the nonlinear vibration perhaps results in printing failure (e.g., snap or tear). Thus, the nonlinear vibration of the membrane with variable velocity should be taken into account.

In current years, various researchers have reviewed more regarding nonlinear vibrational issues pertaining to axial structure of strings, plates, and beams with variable velocities. Nevertheless, the transverse nonlinear vibration of membranes with variable velocities has obtained attention by few scholars. Wickert and Mote [1, 2] investigated transverse vibrations of axially moving strings and beams. The dynamic response of an axially accelerating string was investigated by Pakdemirli and Ulsoy [3], the method of multiple scales was applied to solve the partial differential system. Ravindra and Zhu [4] analyzed nonlinear dynamics of one-mode approximation of an axially moving continuum, the system was modeled as a beam moving with varying speed, and the low-dimensional chaotic response of the system was studied by Melnikov's method. Pakdemirli and Öz [5] and Öz et al. [6] studied a beam with a time-varying axial velocity by using perturbation analysis. Suweken and Van Horssen [7, 8] studied transversal vibrations of a conveyor belt with a low and time-varying velocity. Pellicano [9] reviewed some recent numerical and experimental results regarding the complex dynamics of axially moving systems. The response of axially moving systems was studied by using recent techniques of the nonlinear time series analysis. Pellicano and Vestroni [10] studied nonlinear dynamics and

bifurcation of a simply supported beam subjected to an axial transport of mass by the Galerkin method. The dynamic response of a simply supported travelling beam subjected to a transverse load in the supercritical speed range was investigated by Pellicano and Vestroni [11]. Periodic oscillations were studied by means of continuation techniques, while nonstationary dynamics were investigated through direct simulations. The velocity was presumed as harmonic change that takes place over uniform average speed, which was assumed by Ghayesh [12] and Chen et al. [13], and they used the method of multiple scales and examined nonlinear vibration properties and stability of an axially accelerating string. The findings indicated that the speed changing amplitude and the average speed both had effects on the frequencies and amplitudes. For determining the solution of equations of an axially moving string with time-dependent velocity, two time-scales perturbation method and Laplace transformation technique were used [14]. Ghayesh and Amabili [15] examined the bifurcation diagrams of an axially moving beam, and it was figured out that when the mean axial speed and amplitude of the speed fluctuations changed, the intervals of periodic, quasi-periodic, and chaotic motions took place. Lv et al. [16] used the method of multiple scales and Galerkin truncation for examining the nonlinear dynamic behavior of moving viscoelastic sandwich beams with variable velocities. The effects of average speed, initial tension, and moving speed amplitude on unstable regions and amplitude-frequency response curves were emphasized; consequently a time-dependent speed cannot be ignored in the mathematical modeling. Nguyen et al. [17] considered axial transporting speed as a control input and provided a fresh control algorithm for reducing the influence of transverse vibration through regulating the axial translating speed. Liu et al. [18] presented an ideal deferred feedback control technique for suppressing the nonlinear vibration of an elastic beam with the actuator and piezoelectric sensor. Gong et al. [19] examined the effects of feedback gains, excitation voltage, and damping on the nonlinear vibration properties and amplitude-frequency response of a nanobeam vibrational system. Rezaee and Lotfan [20] evidently expressed that the variation occurring in the axial speed has influence on the slope of "frequency-response" curvatures, when the small-scale effects of axially moving nanoscale beams were considered. Yan and coworkers [21], Mao et al. [22], and Ding et al. [23] examined bifurcation and chaos of a translating beam with pulsating axial velocity, particularly the solution method and modeling were provided. However, 4^{th} order Runge–Kutta algorithm and Galerkin truncation technique were used by them for analyzing the effects of parameter variables on nonlinear behavior of an accelerating viscoelastic beam. Ding and Chen [24] applied the finite difference method to study nonlinear response of axially moving viscoelastic beams. Gafsi et al. [25] analyzed the large deflections of a flexible beam, and a novel strategy was proposed to control the nonlinear vibrations. Breslavsky and Avramov [26] analyzed the effects of boundary condition nonlinearities on free nonlinear vibrations of thin rectangular plates. Avramov and Raimberdiyev [27] investigated lateral vibrations of the beams with two breathing cracks. The stability and bifurcations were also studied. Strozzi and Pellicano [28] studied nonlinear vibrations of functionally graded material (FGM) circular cylindrical shells, and the effects of the geometry (thickness, radius, and length) and material properties on nonlinear dynamics of the shell were highlighted. Liu et al. [29] examined the stability and bifurcations of an axially variable speed plate with large transverse deflections, and the nonlinear dynamic behaviors were studied according to Poincaré map and maximum Lyapunov exponent. Tang and Chen [30, 31] investigated the influence of average in-plane moving speed, viscosity coefficient, in-plane moving speed variation amplitude, and the nonlinear coefficient on the nonlinear vibration of accelerating viscoelastic plates.

Besides, the literature linked to dynamics of a membrane is in abundance, although there is limited literature referring to the nonlinear vibration behavior of the membrane with variable velocity. Marynowski [32, 33] reviewed the nonlinear behavior of the paper web through employing 4^{th} order Runge–Kutta method with the Galerkin method; the viscoelastic beam theory was used to establish the paper web model, and the viscous damping was considered, but the influence of velocity fluctuation was neglected. Lin and Mote [34] formulated the large deflection vibration equations of a moving web; it was shown that the deflection increased with the increase of the translating speed. Luo [35] introduced that nonlinear concept regarding continuous deformational webs and the theory can be used for examining the wrinkling stability of the deformational webs. Banichuk et al. [36] and Ma et al. [37] examined small vibrations and stability of a moving web with nonuniform tension. The undamped nonlinear vibrational response of pretension quadrilateral orthotropic membranes was examined by mathematical and analytical methods in Reference [38]. Soares and Gonçalves [39] investigated the nonlinear dynamic analysis of a stretched hyperelastic membrane subjected to a transversal harmonic force using the shooting method and the finite element technique. Li et al. [40] reviewed the nonliner dynamic response of a membrane under impact load based on the perturbation method and von Kármán's large deformation theory. Free linear vibration properties and stability of a printing paper with variable velocity were discovered by Wu and coworkers [41]; it is shown that the amplitude of pulse speed had influence on the stable region, as well as unstable region of the web. In printing, a time-dependent velocity will affect the printing quality of a membrane, although few authors were attentive towards the effects of variable velocity of membranes on the nonlinear vibration. Thus, our report is focused on the examination of nonlinear parametric vibration of membranes with variable velocity.

In the current research work, the nonlinear vibration characteristics regarding an axially moving membrane with varying velocity are explored through employing the 4^{th} order Runge–Kutta technique and Galerkin method. In addition, chaos and bifurcation behavior of the membrane due to change of mean velocity and velocity pulsation amplitude together with aspect ratio are examined.

2. Establishment of Nonlinear Vibration Equation

Figure 1 is exhibiting the moving membrane with varying velocity, where x is the membrane moving direction, y is the direction that is indicating the width of the membrane, and the z direction is indicating the lateral vibration direction. Axial velocity v_x is assumed as small simple harmonic variations about a constant average axial velocity. Transverse vibration displacement of a membrane is $\overline{w}(x, y, t)$, t represents the time, a is representing the length of a membrane, b is representing the membrane width, T_y and T_x both are the tensions along with membrane's unit length at the edges along y and x directions, $\overline{p}\cos\overline{\omega}t$ is indicating in-plane cosine external excitation per unit area in the z direction, $\overline{p}$ represents the amplitude of external excitation, the surface density is denoted by ρ.

During the instant when lateral vibration of a moving membrane is generated, the absolute velocity vector at all the points within the membrane can be determined as follows:

$$\mathbf{V} = v_x\mathbf{i} + \frac{d\overline{w}}{dt}\mathbf{k}, \tag{1}$$

where $d\overline{w}/dt$ is the speed in the direction of lateral vibration and $\mathbf{i}$ and $\mathbf{k}$ both are indicating the unit vectors along the x and z directions, correspondingly.

The differential operator is expressed as

$$\frac{d}{dt} = \frac{\partial}{\partial t} + v_x\frac{\partial}{\partial x}. \tag{2}$$

The velocity in the transverse vibration direction is expressed as

$$\overline{v}(t) = \frac{d\overline{w}}{dt} = \frac{\partial\overline{w}}{\partial t} + v_x\frac{\partial\overline{w}}{\partial x}. \tag{3}$$

Thereafter, the lateral acceleration is obtained:

$$\begin{aligned}\overline{a} &= \frac{d\overline{v}}{dt} = \frac{\partial\left((\partial\overline{w}/\partial t) + v_x(\partial\overline{w}/\partial x)\right)}{\partial t} + v_x\frac{\partial\left((\partial\overline{w}/\partial t) + v_x(\partial\overline{w}/\partial x)\right)}{\partial x}\\ &= \frac{\partial^2\overline{w}}{\partial t^2} + 2v_x\frac{\partial^2\overline{w}}{\partial t\partial x} + v_x^2\frac{\partial^2\overline{w}}{\partial x^2} + \frac{dv_x}{dt}\cdot\frac{\partial\overline{w}}{\partial x}.\end{aligned} \tag{4}$$

The equilibrium differential equations are given by [36, 42]

$$\begin{cases}\dfrac{\partial N_x}{\partial x} + \dfrac{\partial N_{xy}}{\partial y} = 0,\\[2ex] \dfrac{\partial N_y}{\partial y} + \dfrac{\partial N_{yx}}{\partial x} = 0.\end{cases} \tag{5}$$

where N_x, N_y, and N_{xy} are the membrane inner forces/unit length.

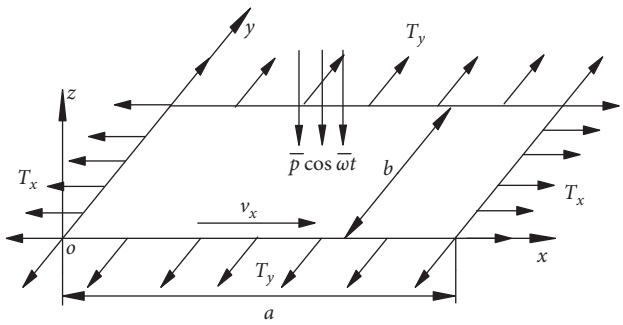

Figure 1: Moving membrane with variable velocity.

Elastic surface differential equation is defined as [42]

$$\begin{aligned}&\rho\left(\frac{\partial^2\overline{w}}{\partial t^2} + 2v_x\frac{\partial^2\overline{w}}{\partial x\partial t} + v_x^2\frac{\partial^2\overline{w}}{\partial x^2}\right) - N_x\frac{\partial^2\overline{w}}{\partial x^2}\\ &- N_y\frac{\partial^2\overline{w}}{\partial y^2} - 2N_{xy}\frac{\partial^2\overline{w}}{\partial x\partial y} = 0.\end{aligned} \tag{6}$$

The membrane is subjected to an external force $\overline{p}\cos\overline{\omega}t$ in the z direction, and the damping effect is taken into account; the forced vibration differential equation of a moving membrane with variable velocity is obtained according to the D'Alembert principle [43]:

$$\begin{aligned}&\rho\left(\frac{\partial^2\overline{w}}{\partial t^2} + 2v_x\frac{\partial^2\overline{w}}{\partial x\partial t} + v_x^2\frac{\partial^2\overline{w}}{\partial x^2} + \frac{dv_x}{dt}\cdot\frac{\partial\overline{w}}{\partial x}\right) - N_x\frac{\partial^2\overline{w}}{\partial x^2}\\ &- N_y\frac{\partial^2\overline{w}}{\partial y^2} - 2N_{xy}\frac{\partial^2\overline{w}}{\partial x\partial y} + \lambda\frac{\partial\overline{w}}{\partial t} = \overline{p}\cos\overline{\omega}t,\end{aligned} \tag{7}$$

where λ is denoting the damping coefficient.

The axial speed of a moving membrane has a simple harmonic fluctuation about the constant mean velocity [29, 30] which can be expressed as follows:

$$v_x = v_0 + v_1\sin\overline{\Omega}t, \quad (v_0, v_1 > 0), \tag{8}$$

where v_0 is denoting the axial average velocity, v_1 represents the change of amplitude with respect to axial velocity, that is, speed pulsation amplitude, and $\overline{\Omega}$ is denoting the frequency of axial velocity.

The nonlinear vibration equation concerning the moving membrane with varying velocity is attained by using von Kármán nonlinear thin plate theory [30]:

$$\begin{cases}\rho\left(\dfrac{\partial^2\overline{w}}{\partial t^2} + 2v_x\dfrac{\partial^2\overline{w}}{\partial x\partial t} + v_x^2\dfrac{\partial^2\overline{w}}{\partial x^2} + \dfrac{dv_x}{dt}\cdot\dfrac{\partial\overline{w}}{\partial x}\right) - N_x\dfrac{\partial^2\overline{w}}{\partial x^2}\\ \quad - N_y\dfrac{\partial^2\overline{w}}{\partial y^2} - 2N_{xy}\dfrac{\partial^2\overline{w}}{\partial x\partial y} + \lambda\dfrac{\partial\overline{w}}{\partial t} - \overline{p}\cos\overline{\omega}t = 0,\\[2ex] \dfrac{\partial^2 N_x}{\partial y^2} + \dfrac{\partial^2 N_y}{\partial x^2} - \mu\dfrac{\partial^2 N_x}{\partial x^2} - \mu\dfrac{\partial^2 N_y}{\partial y^2}\\ \quad = Eh\left[\left(\dfrac{\partial^2\overline{w}}{\partial x\partial y}\right) - \dfrac{\partial^2\overline{w}}{\partial x^2}\dfrac{\partial^2\overline{w}}{\partial y^2}\right],\end{cases} \tag{9}$$

where E is used to denote the elasticity modulus and μ is denoting Poisson's ratio.

The internal force of the membranes N_x, N_y, and N_{xy} can be represented with help of the Airy stress function Φ [36]:

$$N_x = \frac{\partial^2 \Phi}{\partial y^2},$$
$$N_y = \frac{\partial^2 \Phi}{\partial x^2}, \tag{10}$$
$$N_{xy} = -\frac{\partial^2 \Phi}{\partial x \partial y}.$$

The equilibrium differential equations of the membrane units are independent from each other, the membrane is soft and homogeneous, and the effect of shear stress on the vibration of the membrane is smaller; therefore, we can assume $N_{xy} = 0$, so the boundary conditions of the membrane are obtained:

$$N_x\big|_{x=0,a} = T_x,$$
$$N_y\big|_{y=0,b} = T_y, \tag{11}$$
$$N_{xy} = 0.$$

Then, equation (9) can be defined as follows:

$$\begin{cases} \rho\left(\dfrac{\partial^2 \overline{w}}{\partial t^2} + 2v_x \dfrac{\partial^2 \overline{w}}{\partial x \partial t} + v_x^2 \dfrac{\partial^2 \overline{w}}{\partial x^2} + \dfrac{dv_x}{dt} \cdot \dfrac{\partial \overline{w}}{\partial x}\right) \\ \quad - \dfrac{\partial^2 \Phi}{\partial y^2} \dfrac{\partial^2 \overline{w}}{\partial x^2} - \dfrac{\partial^2 \Phi}{\partial x^2} \dfrac{\partial^2 \overline{w}}{\partial y^2} + \lambda \dfrac{\partial \overline{w}}{\partial t} = \overline{p} \cos \overline{\omega} t, \\ \dfrac{\partial^4 \Phi}{\partial x^4} + \dfrac{\partial^4 \Phi}{\partial y^4} = Eh\left[\left(\dfrac{\partial^2 \overline{w}}{\partial x \partial y}\right)^2 - \dfrac{\partial^2 \overline{w}}{\partial x^2} \dfrac{\partial^2 \overline{w}}{\partial y^2}\right]. \end{cases} \tag{12}$$

Substituting equation (8) into equation (12) yields

$$\begin{cases} \rho\left[\dfrac{\partial^2 \overline{w}}{\partial t^2} + 2\left(v_0 + v_1 \sin \overline{\Omega} t\right) \dfrac{\partial^2 \overline{w}}{\partial x \partial t} + \left(v_0 + v_1 \sin \overline{\Omega} t\right)^2 \dfrac{\partial^2 \overline{w}}{\partial x^2}\right. \\ \quad \left. + \overline{\Omega} v_1 \cos \overline{\Omega} t \dfrac{\partial \overline{w}}{\partial x}\right] - \dfrac{\partial^2 \Phi}{\partial y^2} \dfrac{\partial^2 \overline{w}}{\partial x^2} - \dfrac{\partial^2 \Phi}{\partial x^2} \dfrac{\partial^2 \overline{w}}{\partial y^2} \\ \quad + \lambda \dfrac{\partial \overline{w}}{\partial t} - \overline{p} \cos \overline{\omega} t = 0, \\ \dfrac{\partial^4 \Phi}{\partial x^4} + \dfrac{\partial^4 \Phi}{\partial y^4} = Eh\left[\left(\dfrac{\partial^2 \overline{w}}{\partial x \partial y}\right)^2 - \dfrac{\partial^2 \overline{w}}{\partial x^2} \dfrac{\partial^2 \overline{w}}{\partial y^2}\right]. \end{cases} \tag{13}$$

Let the dimensionless quantities be expressed as

$$\xi = \frac{x}{a},$$
$$\eta = \frac{y}{b},$$
$$w = \frac{\overline{w}}{h},$$
$$\tau = t\sqrt{\frac{Eh^3}{\rho a^4}},$$
$$c = v\sqrt{\frac{\rho a^2}{Eh^3}},$$
$$c_1 = v_1\sqrt{\frac{\rho a^2}{Eh^3}},$$
$$r = \frac{a}{b}, \tag{14}$$
$$f = \frac{\Phi}{Eh^3},$$
$$\Omega = \overline{\Omega}\sqrt{\frac{\rho a^4}{Eh^3}},$$
$$p = \overline{p}\frac{a^4}{Eh^3},$$
$$\omega = \overline{\omega}\sqrt{\frac{\rho a^4}{Eh^3}},$$
$$\gamma = \lambda\sqrt{\frac{a^4}{\rho Eh^3}},$$

where r is the aspect ratio, c is the dimensionless average speed, c_1 is representing the dimensionless amplitude of pulsating speed, and p is the dimensionless external excitation amplitude. The dimensionless nonlinear governing equations of the axially accelerating moving membrane can be achieved as follows:

$$\begin{cases} \dfrac{\partial^2 w}{\partial \tau^2} + 2\left(c + c_1 \sin \Omega \tau\right) \dfrac{\partial^2 w}{\partial \xi \partial \tau} \\ \quad + \left(c^2 + 2cc_1 \sin \Omega \tau + c_1^2 \sin^2 \Omega \tau\right) \dfrac{\partial^2 w}{\partial \xi^2} + \Omega c_1 \cos \Omega \tau \dfrac{\partial w}{\partial \xi} \\ \quad - r^2 \dfrac{\partial^2 f}{\partial \eta^2} \dfrac{\partial^2 w}{\partial \xi^2} - r^2 \dfrac{\partial^2 f}{\partial \xi^2} \dfrac{\partial^2 w}{\partial \eta^2} + \gamma \dfrac{\partial w}{\partial \tau} = p \cos \omega \tau, \\ \dfrac{\partial^4 f}{\partial \xi^4} + r^4 \dfrac{\partial^4 f}{\partial \eta^4} = r^2\left(\dfrac{\partial^2 w}{\partial \xi \partial \eta}\right)^2 - r^2 \dfrac{\partial^2 w}{\partial \xi^2} \dfrac{\partial^2 w}{\partial \eta^2}. \end{cases} \tag{15}$$

The boundary conditions of nonlinear vibration membrane can be determined as [44]

$$\left.\frac{\partial^2 f}{\partial \eta^2}\right|_{\xi=0,1} = 1,$$
$$\left.\frac{\partial^2 f}{\partial \xi \partial \eta}\right|_{\xi=0,1} = 0,$$
$$w = 0,$$
$$\left.\frac{\partial^2 f}{\partial \xi^2}\right|_{\eta=0,1} = 1,$$
$$\left.\frac{\partial^2 f}{\partial \xi \partial \eta}\right|_{\eta=0,1} = 0,$$
$$w = 0. \tag{16}$$

3. Separation of the Variables

The displacement function satisfying the boundary conditions can be expressed as follows:

$$w(\xi, \eta, \tau) = \sum_{i=1}^{M_i} \sum_{j=1}^{M_j} q_{ij}(\tau) \sin(i\pi\xi) \sin(j\pi\eta). \tag{17}$$

It is sufficient for reflecting the response characteristics of the system when $M_i = 2$ and $M_j = 1$ [29, 45]:

$$\begin{aligned} w(\xi, \eta, t) &= \sum_{i=1}^{2} q_{i1}(\tau) \sin(i\pi\xi) \sin(\pi\eta) \\ &= q_{11}(\tau) \sin(\pi\xi) \sin(\pi\eta) + q_{21}(\tau) \sin(2\pi\xi) \sin(\pi\eta). \end{aligned} \tag{18}$$

The inner force function satisfying the boundary conditions can be expressed as follows [45]:

$$f(\xi, \eta, \tau) = \frac{\xi^2}{2} + \frac{\eta^2}{2} + \sum_{i=1}^{M_i} \sum_{j=1}^{M_j} f_{ij}(\tau) \sin^2(i\pi\xi) \sin^2(j\pi\eta), \tag{19}$$

where $f_{ij}(\tau)$ is the undetermined coefficient.

When $i = 1$ and $j = 1$ and $i = 2$ and $j = 1$, the inner force function $f(\xi, \eta, t)$ can be determined as follows [45]:

$$\begin{aligned} f(\xi, \eta, \tau) = \frac{\xi^2}{2} + \frac{\eta^2}{2} &+ f_{11}(\tau) \sin^2(\pi\xi) \sin^2(\pi\eta) \\ &+ f_{21}(\tau) \sin^2(2\pi\xi) \sin^2(\pi\eta), \end{aligned} \tag{20}$$

where $f_{11}(\tau)$ and $f_{21}(\tau)$ are the undetermined coefficients.

According to the Galerkin method, substituting equations (18) and (20) into equation (15) produces

$$\begin{aligned} \int_0^1 \int_0^1 \left[\frac{\partial^4 f}{\partial \xi^4} + r^4 \frac{\partial^4 f}{\partial \eta^4} - r^2 \left(\frac{\partial^2 w}{\partial \xi \partial \eta} \right)^2 + r^2 \frac{\partial^2 w}{\partial \xi^2} \frac{\partial^2 w}{\partial \eta^2} \right] \sin^2(i\pi\xi) \\ \cdot \sin^2(j\pi\eta) d\xi \, d\eta = 0. \end{aligned} \tag{21}$$

Performing two integrations on (21) when $i = 1$ and $j = 1$ and $i = 2$ and $j = 1$, correspondingly, then we obtain

$$\begin{aligned} &\left(6 + 6r^4\right) f_{11}(\tau) + 4r^4 f_{21}(\tau) + r^2 q_{11}^2(\tau) \\ &\quad + 2r^2 q_{21}^2(\tau) = 0, \\ &8r^4 f_{11}(\tau) + \left(192 + 12r^4\right) f_{21}(\tau) + r^2 q_{11}^2(\tau) \\ &\quad + 8r^2 q_{21}^2(\tau) = 0. \end{aligned} \tag{22}$$

$f_{11}(\tau)$ and $f_{21}(\tau)$ are signified as follows:

$$\begin{aligned} f_{11}(\tau) &= \frac{-\left(96r^2 + 4r^6\right) q_{11}^2(\tau) - \left(192r^2 - 4r^6\right) q_{21}^2(\tau)}{20r^8 + 612r^4 + 576} \\ &= \left[\beta \left[\alpha_{11} q_{11}^2(\tau) + \alpha_{12} q_{21}^2(\tau)\right]\right], \\ f_{21}(\tau) &= \frac{\left(r^6 - 3r^2\right) q_{11}^2(\tau) - \left(16r^6 + 24r^2\right) q_{21}^2(\tau)}{20r^8 + 612r^4 + 576} \\ &= \beta \left[\alpha_{21} q_{11}^2(\tau) + \alpha_{22} q_{21}^2(\tau)\right], \end{aligned} \tag{23}$$

where

$$\begin{aligned} \alpha_{11} &= -\left(96r^2 + 4r^6\right), \\ \alpha_{12} &= 4r^6 - 192r^2, \\ \alpha_{21} &= r^6 - 3r^2, \\ \alpha_{22} &= -\left(16r^6 + 24r^2\right), \\ \beta &= \frac{1}{20r^8 + 612r^4 + 576}. \end{aligned} \tag{24}$$

Substituting equations (18) and (20) into equation (15) generates the subsequent equations by employing the Galerkin method:

$$\begin{aligned} \int_0^1 \int_0^1 \Bigg[&\frac{\partial^2 w}{\partial \tau^2} + 2\left(c + c_1 \sin \Omega\tau\right) \frac{\partial^2 w}{\partial \xi \partial \tau} \\ &+ \left(c^2 + 2cc_1 \sin \Omega\tau + c_1^2 \sin^2 \Omega\tau\right) \frac{\partial^2 w}{\partial \xi^2} + \Omega c_1 \cos \Omega\tau \frac{\partial w}{\partial \xi} \\ &- r^2 \frac{\partial^2 f}{\partial \eta^2} \frac{\partial^2 w}{\partial \xi^2} - r^2 \frac{\partial^2 f}{\partial \xi^2} \frac{\partial^2 w}{\partial \eta^2} + \gamma \frac{\partial w}{\partial \tau} - p \cos \omega\tau \Bigg] \\ &\cdot \sin(m\pi\xi) \sin(\pi\eta) d\xi \, d\eta = 0. \end{aligned} \tag{25}$$

The state equations of the moving membrane system with varying velocity when $m = 1$ and $m = 2$ can be described as follows:

$$\begin{aligned} \ddot{q}_{11} + G_{11}\dot{q}_{21} + \gamma \dot{q}_{11} + k_{11} q_{11} + k_{12} q_{21} + k_{13} q_{11}^3 \\ + k_{14} q_{11} q_{21}^2 = Q \cos(\omega t), \end{aligned} \tag{26}$$

$$\begin{aligned} \ddot{q}_{21} + G_{21}\dot{q}_{11} + \gamma \dot{q}_{21} + k_{21} q_{11} + k_{22} q_{21} \\ + k_{23} q_{21}^3 + k_{24} q_{11}^2 q_{21} = 0, \end{aligned} \tag{27}$$

where

$$
\begin{aligned}
G_{11} &= -\frac{16\left(c + c_1 \sin \Omega\tau\right)}{3},\\
k_{11} &= 2\pi^2 r^2 - \pi^2\left(c^2 + 2cc_1 \sin \Omega\tau + c_1^2 \sin^2 \Omega\tau\right),\\
k_{12} &= -\frac{8\Omega c_1 \cos \Omega\tau}{3},\\
k_{13} &= -\frac{\pi^4 r^2 \beta}{2}\left(3\alpha_{11} + \alpha_{21}\right),\\
k_{14} &= -\frac{\pi^4 r^2 \beta}{2}\left(3\alpha_{12} + \alpha_{22}\right),\\
Q &= \frac{16\mathrm{p}}{\pi^2},\\
G_{21} &= \frac{16\left(c + c_1 \sin \Omega\tau\right)}{3},\\
k_{21} &= \frac{8\Omega c_1 \cos \Omega\tau}{3},\\
k_{22} &= 5\pi^2 r^2 - 4\pi^2\left(c^2 + 2cc_1 \sin \Omega\tau + c_1^2 \sin^2 \Omega\tau\right),\\
k_{23} &= -2\pi^4 r^2 \beta\left(\alpha_{12} + 3\alpha_{22}\right),\\
k_{24} &= -2\pi^4 r^2 \beta\left(\alpha_{11} + 3\alpha_{21}\right).
\end{aligned}
\tag{28}
$$

Introducing the following parameter variables:

$$
\begin{aligned}
X_1 &= q_{11},\\
X_3 &= q_{21},\\
X_2 &= \dot{X}_1,\\
X_4 &= \dot{X}_3,
\end{aligned}
\tag{29}
$$

Equations (26) and (27) can be expressed as follows:

$$
\begin{aligned}
\dot{X}_2 &= -G_{11}X_4 - \gamma X_2 - k_{11}X_1 - k_{12}X_3 - k_{13}X_1^3\\
&\quad - k_{14}X_1X_3^2 + Q\cos\left(\omega t\right),\\
\dot{X}_4 &= -G_{21}X_2 - \gamma X_4 - k_{21}X_1 - k_{22}X_3 - k_{23}X_3^3 - k_{24}X_3X_1^2,
\end{aligned}
\tag{30}
$$

where γ is representing the dimensionless damping coefficient.

4. Numerical Analysis

The 4th order Runge–Kutta technique was used for mathematically solving the state equation of the moving membrane structure. In this way, the association between dynamic characteristics of the system, velocity pulsating amplitude, average velocity, and aspect ratio are obtained. For the purpose of revealing the nonlinear dynamic characteristics of the system, Poincaré maps, bifurcation graphs, phase-plane diagrams, and time histories were used [32, 33, 46]. The study is based on the commonly used parameters of the printing membrane.

4.1. Effects of Velocity Pulsation Amplitude on Nonlinear Vibration Characteristics. As it is exhibited in Figure 2, the displacement bifurcation graph of dimensionless velocity pulsation amplitude when the frequency of dimensionless velocity $\Omega = 2$, average speed $c = 0.5$, dimensionless excitation frequency $\omega = 1$, dimensionless external excitation amplitude $p = 10$, and dimensionless damping constant $\gamma = 0.05$, the aspect ratio $r = 0.5$, and the initial values are [0.01, 0, 0.01, 0], the range of velocity pulsation amplitude is $0.01 \le c_1 \le 0.35$. Figure 2 indicates that when $0.01 \le c_1 < 0.195$, the bifurcation graph resembles fewer points, the membrane is in a periodic motion, and it is demonstrated that the membrane is in stable motion in this region. When $0.195 \le c_1 \le 0.35$, the bifurcation graph is showing the irregular dense point, and it is observed that membrane is in chaotic motion, and membrane is in the unstable motion state at these points. Therefore, as there is larger dimensionless velocity pulsation amplitude, eventually it gives rise to the more obvious nonlinear vibration phenomenon and results in easier instability. Generally, the system moves from periodic motion to chaotic motion.

Figure 3 shows the displacement bifurcation graph of dimensionless velocity pulsation amplitude when the parameters are $\Omega = 2$, $c = 0.5$, $\omega = 1$, $p = 10$, $\gamma = 0.05$, $r = 0.5$, and the initial value is [0.05, 0, 0.05, 0]. As it can be observed from Figures 2 and 3, the system motion process is remarkably different because of different initial values. It is found that the nonlinear vibration characteristics of membranes are sensitive to the initial conditions.

4.2. Effects of Mean Velocity on Nonlinear Vibration Characteristics. Figure 4 shows the displacement bifurcation graph of dimensionless average velocity when the parameters are $\Omega = 2$, $c_1 = 0.05$, $\omega = 1$, p = 10, $\gamma = 0.1$, $r = 0.5$, and the initial value is [0.01, 0, 0.01, 0]. The range of dimensionless velocity is $0.01 \le c \le 1$. Figure 4 shows that when $0.01 \le c < 0.66$ and $0.67 < c < 0.71$, the bifurcation graph resembles fewer points, and it is specified that membrane is in stable motion in these regions. When $0.66 \le c \le 0.67$ and $0.71 < c \le 1$, the bifurcation graph shows the dense points, and it is observed that the membrane is in chaotic motion, and the membrane is unstable in these regions. Therefore, as there is larger dimensionless velocity, faster would be the instability.

Figures 5–7 are all about phase-plane diagrams, Poincaré maps, and time histories when $c = 0.65$, $c = 0.658$, and $c = 0.665$, correspondingly.

The phase-plane curve has a steady sealed graphic when $c = 0.65$, and the Poincaré map possesses two points; it is shown that the overall structure is in the periodic motion. The phase-plane curve possesses many steady sealed graphics, whereas the Poincaré map has a circle of discrete points, when $c = 0.658$, and it is shown that the system is in quasi-periodic motion. When $c = 0.665$, the phase-plane curve is not closed, the Poincaré maps possess lots of unstable dense points, and it is observed that the overall system is in chaotic motion. It summarizes that, with the rise of dimensionless velocity c, the system from the periodic

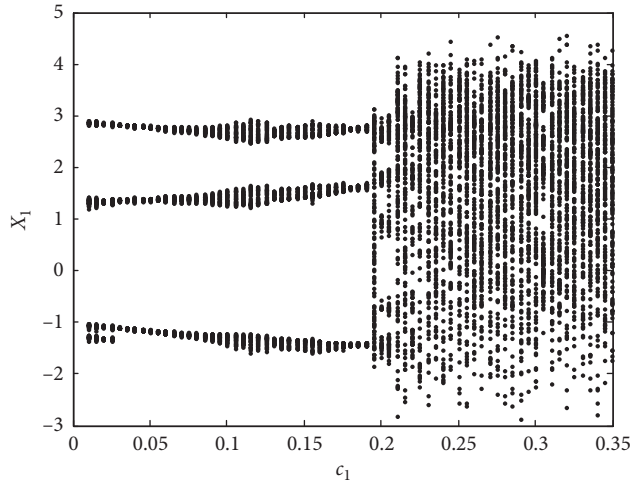

Figure 2: The displacement bifurcation graph of velocity pulsation amplitude ($\Omega = 2$, $\omega = 1$, $\gamma = 0.05$, $r = 0.5$, $p = 10$, $c = 0.5$, and the initial value is [0.01, 0, 0.01, 0]).

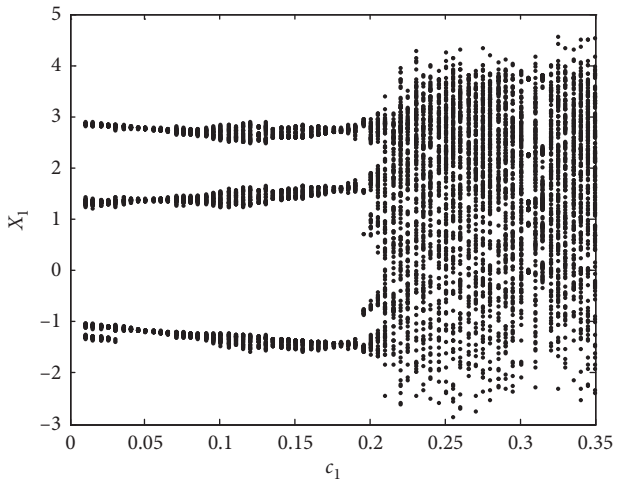

Figure 3: The displacement bifurcation graph of velocity pulsation amplitude ($\Omega = 2$, $\omega = 1$, $\gamma = 0.05$, $r = 0.5$, $p = 10$, $c = 0.5$, and the initial value is [0.05, 0, 0.05, 0]).

motion transforms into quasi-periodic motion and later on enters into chaotic motion.

4.3. Effects of Aspect Ratio on Stability. It is displayed in Figure 8 that the bifurcation diagram of dimensionless displacement and aspect ratio when the frequency of dimensionless velocity $\Omega = 2$, dimensionless velocity pulsation amplitude $c_1 = 0.05$, dimensionless excitation frequency $\omega = 1$, dimensionless damping constant $\gamma = 0.05$, dimensionless speed $c = 0.5$, dimensionless external excitation amplitude $p = 10$, and the initial values are [0.01, 0, 0.01, 0], the range of variation of aspect ratio is $0.2 \le r \le 2$. As it is shown in Figure 8, when $0.305 < r < 0.355$ and $0.395 < r \le 2$, the bifurcation diagram has fewer points, and it is specified that the membrane is in stable motion in these regions; thus the membrane is in steady working range. When $0.2 \le r \le 0.305$, $0.355 \le r \le 0.395$, the bifurcation figure has the dense points,

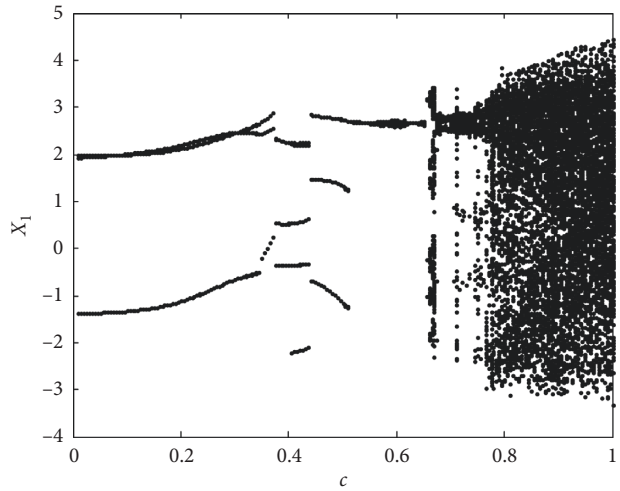

Figure 4: The displacement bifurcation graph of mean speed ($\Omega = 2$, $\omega = 1$, $\gamma = 0.1$, $r = 0.5$, $p = 10$, $c_1 = 0.05$, and the initial value is [0.01, 0, 0.01, 0]).

and it is observed that membrane is in chaotic motion. Thus, in these regions, the nonlinear vibrational incidence is apparent, and the membrane is in the unstable state. In summary, when the aspect ratio will increase, the membrane will become more stable.

5. Conclusions

The nonlinear vibration characteristics of the membrane in motion with varying velocity are reviewed. The results are discussed as follows:

(1) The nonlinear vibration characteristics of a membrane are sensitive to the initial motion conditions.

(2) When dimensionless velocity pulsation amplitude is a control parameter, the membrane is supposed to be in the stable working condition in the region of $0.01 \le c_1 < 0.195$; the membrane is unstable in the region of $0.195 \le c_1 \le 0.35$. Besides, the chaos is prominent with the increase of the dimensionless velocity pulsation amplitude, together with this irregularity can take place easily; therefore, we can efficiently control the chaos phenomenon through reducing the dimensionless velocity pulsation amplitude.

(3) When the dimensionless average velocity is variable, the membrane is supposed to be in the condition of steady working region, in the regions of $0.01 \le c < 0.66$ and $0.67 < c < 0.71$, and the membrane is unstable in the regions of $0.66 \le c \le 0.67$ and $0.71 < c \le 1$. Furthermore, the higher the dimensionless average velocity is, the more prominent will be the chaos motion, and the instability can take place with relative ease; thus, we can efficiently control the chaos phenomenon through reducing the dimensionless average velocity.

(4) When the aspect ratio is used as a control parameter, the membrane is supposed to be in the stable

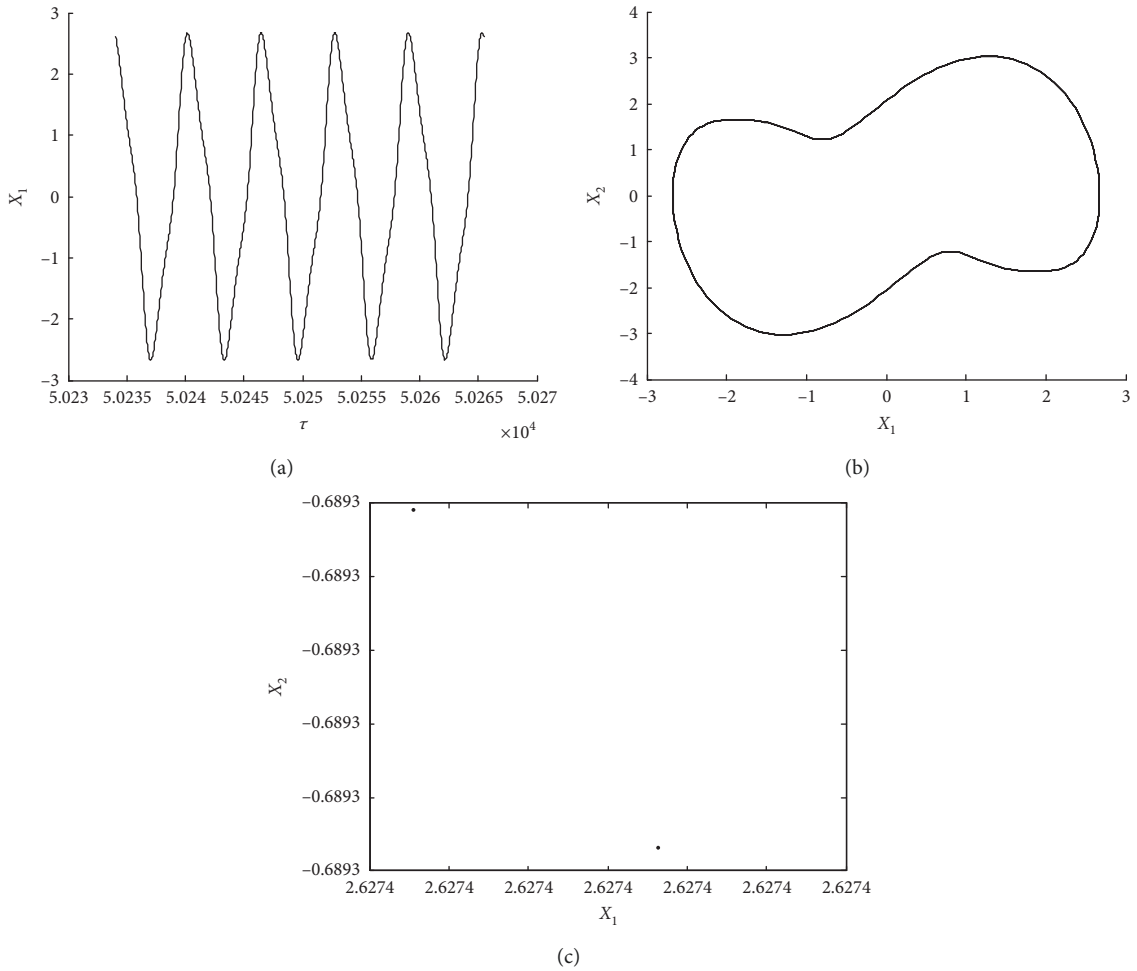

Figure 5: The periodic motion ($\Omega = 2$, $\omega = 1$, $\gamma = 0.1$, $r = 0.5$, $p = 10$, $c_1 = 0.05$, and $c = 0.65$). (a) Time histories. (b) Phase-plane diagrams. (c) Poincaré maps.

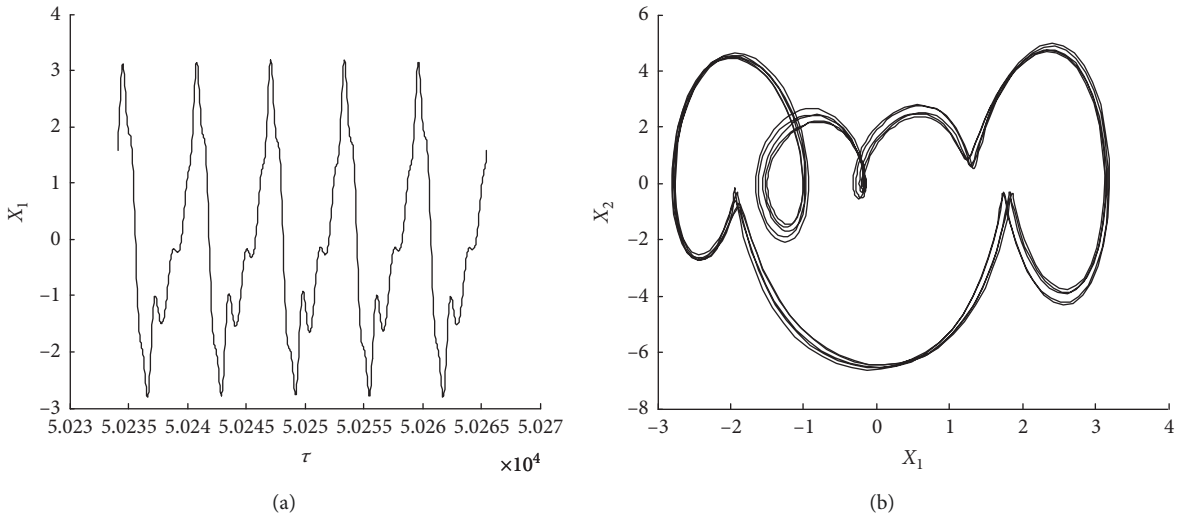

Figure 6: Continued.

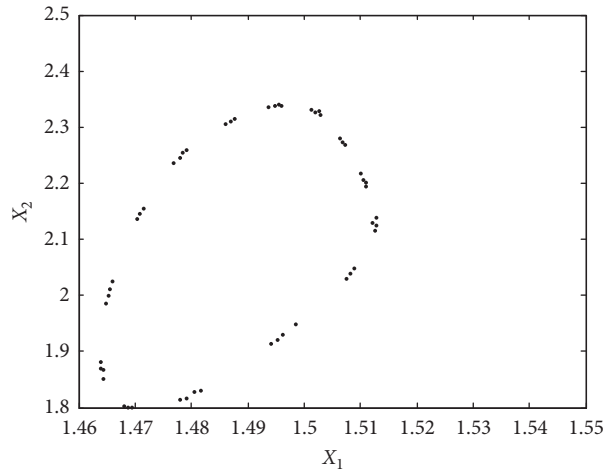

(c)

FIGURE 6: The quasi-periodic motion ($\Omega = 2$, $\omega = 1$, $\gamma = 0.1$, $r = 0.5$, $p = 10$, $c_1 = 0.05$, and $c = 0.658$). (a) Time histories. (b) Phase-plane diagrams. (c) Poincaré maps.

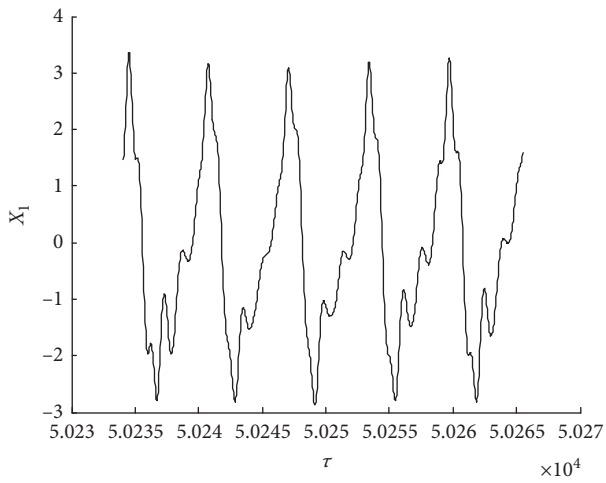

(a)

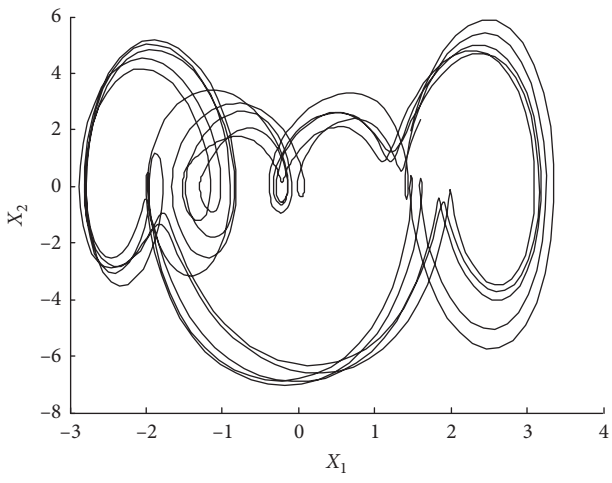

(b)

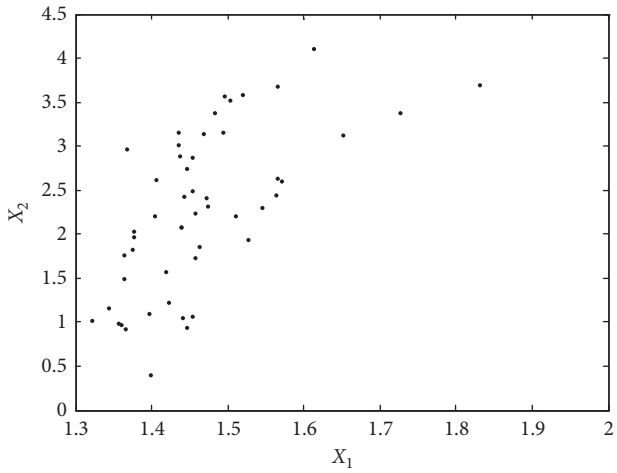

(c)

FIGURE 7: The chaotic motion ($\Omega = 2$, $\omega = 1$, $\gamma = 0.1$, $r = 0.5$, $p = 10$, $c_1 = 0.05$, and $c = 0.665$). (a) Time histories. (b) Phase-plane diagrams. (c) Poincaré maps.

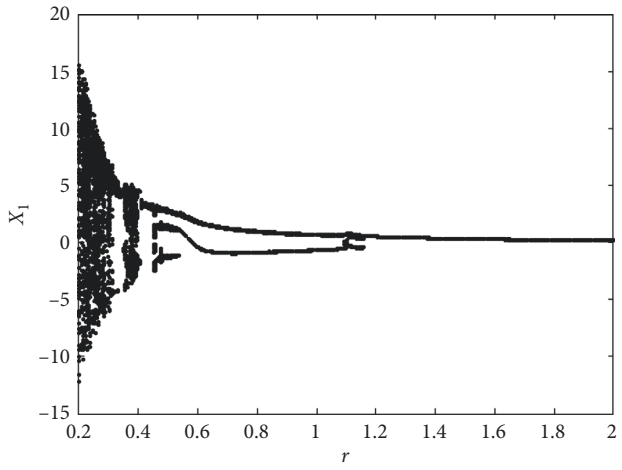

Figure 8: The displacement bifurcation diagram of the aspect ratio ($\Omega = 2$, $\omega = 1$, $\gamma = 0.05$, $c_1 = 0.05$, and $c = 0.5$).

working condition in regions of $0.305 < r < 0.355$ and $0.395 < r \leq 2$, and the membrane is unstable in the regions of $0.2 \leq r \leq 0.305$ and $0.355 \leq r \leq 0.395$. The findings indicated that the system is highly unstable with the decrease of the aspect ratio. Thus, with the increase in the aspect ratio, we can efficiently control possible stability issues owning to stronger nonlinear phenomenon.

(5) Note that, in this paper, there are truncation errors (formula (17)). In practical applications, the limited terms of formula (17) are retained for different needs of the problem. However, we should discuss that how accurately the numerical results for the ODEs are approximating the solutions of the PDEs and these are hard questions.

Data Availability

All the data used to support the findings of this study are already included within the manuscript.

Conflicts of Interest

The authors declare that there are no conflicts of interest regarding the publication of this article.

Acknowledgments

The authors thankfully confess the support of the Natural Science Foundation of Shaanxi Province (nos. 2018JM5023, 2018JM1028, and 2018JM5119), the Ph.D. Innovation fund projects of Xi'an University of Technology (no. 310-252071702), and the National Natural Science Foundation of China (no. 51705420).

References

[1] J. A. Wickert and C. D. Mote, "Travelling load response of an axially moving string," *Journal of Sound and Vibration*, vol. 149, no. 2, pp. 267–284, 1991.

[2] J. A. Wickert and C. D. Mote, "Response and discretization methods for axially moving materials," *Applied Mechanics Reviews*, vol. 44, pp. 279–284, 1991.

[3] M. Pakdemirli and A. G. Ulsoy, "Stability analysis of an axially accelerating string," *Journal of Sound and Vibration*, vol. 203, no. 5, pp. 815–832, 1997.

[4] B. Ravindra and W. D. Zhu, "Low-dimensional chaotic response of axially accelerating continuum in the supercritical regime," *Archive of Applied Mechanics*, vol. 68, no. 3-4, pp. 195–205, 1998.

[5] M. Pakdemirli and H. R. Öz, "Infinite mode analysis and truncation to resonant modes of axially accelerated beam vibrations," *Journal of Sound and Vibration*, vol. 311, no. 3–5, pp. 1052–1074, 2008.

[6] H. R. Öz, M. Pakdemirli, and H. Boyacı, "Non-linear vibrations and stability of an axially moving beam with time-dependent velocity," *International Journal of Non-Linear Mechanics*, vol. 36, no. 1, pp. 107–115, 2001.

[7] G. Suweken and W. T. Van Horssen, "On the transversal vibrations of a conveyor belt with a low and time-varying velocity. Part II: the beam-like case," *Journal of Sound and Vibration*, vol. 267, no. 5, pp. 1007–1027, 2003.

[8] G. Suweken and W. T. Van Horssen, "On the weakly nonlinear, transversal vibrations of a conveyor belt with a low and time-varying velocity," *Nonlinear Dynamics*, vol. 31, no. 2, pp. 197–223, 2003.

[9] F. Pellicano, "On the dynamic properties of axially moving systems," *Journal of Sound and Vibration*, vol. 281, no. 3–5, pp. 593–609, 2005.

[10] F. Pellicano and F. Vestroni, "Nonlinear dynamics and bifurcations of an axially moving beam," *Journal of Vibration and Acoustics*, vol. 122, no. 1, pp. 21–30, 2000.

[11] F. Pellicano and F. Vestroni, "Complex dynamics of high-speed axially moving systems," *Journal of Sound and Vibration*, vol. 258, no. 1, pp. 31–44, 2002.

[12] M. H. Ghayesh, "Parametric vibrations and stability of an axially accelerating string guided by a non-linear elastic foundation," *International Journal of Non-Linear Mechanics*, vol. 45, no. 4, pp. 382–394, 2010.

[13] L.-Q. Chen, Y.-Q. Tang, and J. W. Zu, "Nonlinear transverse vibration of axially accelerating strings with exact internal resonances and longitudinally varying tensions," *Nonlinear Dynamics*, vol. 76, no. 2, pp. 1443–1468, 2014.

[14] R. A. Malookani and W. T. van Horssen, "On resonances and the applicability of Galerkin's truncation method for an axially moving string with time-varying velocity," *Journal of Sound and Vibration*, vol. 344, pp. 1–17, 2015.

[15] M. H. Ghayesh and M. Amabili, "Steady-state transverse response of an axially moving beam with time-dependent axial speed," *International Journal of Non-Linear Mechanics*, vol. 49, pp. 40–49, 2013.

[16] H.-W. Lv, L. Li, and Y.-H. Li, "Non-linearly parametric resonances of an axially moving viscoelastic sandwich beam with time-dependent velocity," *Applied Mathematical Modelling*, vol. 53, pp. 83–105, 2018.

[17] Q. C. Nguyen, K.-S. Hong, and S. S. Ge, "Transverse vibration control of axially moving beams by regulation of axial velocity," *IFAC Proceedings Volumes*, vol. 44, no. 1, pp. 5579–5584, 2011.

[18] C. Liu, S. Yue, and J. Zhou, "Piezoelectric optimal delayed feedback control for nonlinear vibration of beams," *Journal of Low Frequency Noise, Vibration and Active Control*, vol. 35, no. 1, pp. 25–38, 2016.

[19] Q. Gong, C. Liu, Y. Xu et al., "Nonlinear vibration control with nanocapacitive sensor for electrostatically actuated nanobeam," *Journal of Low Frequency Noise, Vibration and Active Control*, vol. 37, no. 2, pp. 235–252, 2018.

[20] M. Rezaee and S. Lotfan, "Non-linear nonlocal vibration and stability analysis of axially moving nanoscale beams with time-dependent velocity," *International Journal of Mechanical Sciences*, vol. 96-97, pp. 36–46, 2015.

[21] Q.-Y. Yan, H. Ding, and L.-Q. Chen, "Periodic responses and chaotic behaviors of an axially accelerating viscoelastic Timoshenko beam," *Nonlinear Dynamics*, vol. 78, no. 2, pp. 1577–1591, 2014.

[22] X.-Y. Mao, H. Ding, and L.-Q. Chen, "Parametric resonance of a translating beam with pulsating axial speed in the supercritical regime," *Mechanics Research Communications*, vol. 76, pp. 72–77, 2016.

[23] H. Ding, Q. Y. Yan, and L. Q. Chen, "Chaotic dynamics in the forced nonlinear vibration of an axially accelerating viscoelastic beam," *Acta Physica Sinica*, vol. 62, no. 20, article 200502, 2013.

[24] H. Ding and L. Q. Chen, "Nonlinear models for transverse forced vibration of axially moving viscoelastic beams," *Shock and Vibration*, vol. 18, no. 1-2, pp. 281–287, 2011.

[25] W. Gafsi, F. Najar, S. Choura, and S. El-Borgi, "Confinement of vibrations in variable-geometry nonlinear flexible beam," *Shock and Vibration*, vol. 2014, Article ID 687340, 7 pages, 2014.

[26] I. D. Breslavsky and K. V. Avramov, "Effect of boundary condition nonlinearities on free large-amplitude vibrations of rectangular plates," *Nonlinear Dynamics*, vol. 74, no. 3, pp. 615–627, 2013.

[27] K. Avramov and T. Raimberdiyev, "Bifurcations behavior of bending vibrations of beams with two breathing cracks," *Engineering Fracture Mechanics*, vol. 178, pp. 22–38, 2017.

[28] M. Strozzi and F. Pellicano, "Nonlinear vibrations of functionally graded cylindrical shells," *Thin-Walled Structures*, vol. 67, pp. 63–77, 2013.

[29] J. T. Liu, X. D. Yang, and B. C. Wen, "Nonlinear dynamic behaviors of an axially accelerating large deflection thin plate," *Journal of Vibration and Shock*, vol. 31, pp. 11–15, 2012, in Chinese.

[30] Y.-Q. Tang and L.-Q. Chen, "Parametric and internal resonances of in-plane accelerating viscoelastic plates," *Acta Mechanica*, vol. 223, no. 2, pp. 415–431, 2012.

[31] Y. Tang, D. Zhang, M. Rui, X. Wang, and D. Zhu, "Dynamic stability of axially accelerating viscoelastic plates with longitudinally varying tensions," *Applied Mathematics and Mechanics*, vol. 37, no. 12, pp. 1647–1668, 2016.

[32] K. Marynowski, "Non-linear vibrations of an axially moving viscoelastic web with time-dependent tension," *Chaos, Solitons & Fractals*, vol. 21, no. 2, pp. 481–490, 2004.

[33] K. Marynowski, "Non-linear vibrations of the axially moving paper web," *Journal of Theoretical & Applied Mechanics*, vol. 46, no. 3, pp. 565–580, 2008.

[34] C. C. Lin and C. D. Mote, "Equilibrium displacement and stress distribution in a two-dimensional, axially moving web under transverse loading," *Journal of Applied Mechanics*, vol. 62, no. 3, pp. 772–779, 1995.

[35] A. C. J. Luo, "A theory for nonlinear soft webs," *Communications in Nonlinear Science and Numerical Simulation*, vol. 16, no. 4, pp. 2184–2199, 2011.

[36] N. Banichuk, J. Jeronen, P. Neittaanmäki, T. Saksa, and T. Tuovinen, "Theoretical study on travelling web dynamics and instability under non-homogeneous tension," *International Journal of Mechanical Sciences*, vol. 66, pp. 132–140, 2013.

[37] L. Ma, J. Chen, W. Tang, and Z. Yin, "Transverse vibration and instability of axially travelling web subjected to non-homogeneous tension," *International Journal of Mechanical Sciences*, vol. 133, pp. 752–758, 2017.

[38] C. Liu, Z. Zheng, and X. Yang, "Analytical and numerical studies on the nonlinear dynamic response of orthotropic membranes under impact load," *Earthquake Engineering and Engineering Vibration*, vol. 15, no. 4, pp. 657–672, 2016.

[39] R. M. Soares and P. B. Gonçalves, "Nonlinear vibrations and instabilities of a stretched hyperelastic annular membrane," *International Journal of Solids & Structures*, vol. 49, no. 3-4, pp. 514–526, 2012.

[40] D. Li, Z. Zheng, Y. Tian, J. Sun, X. He, and Y. Lu, "Stochastic nonlinear vibration and reliability of orthotropic membrane structure under impact load," *Thin-Walled Structures*, vol. 119, pp. 247–255, 2017.

[41] J. Wu, Q. Wu, L. e. Ma, and L. Liu, "Parameter vibration and dynamic stability of the printing paper web with variable speed," *Journal of Low Frequency Noise, Vibration and Active Control*, vol. 29, no. 4, pp. 281–291, 2010.

[42] Z. L. Xu, *Elastic Mechanics (Part II)*, Higher Education Press, Beijing, China, 2015, in Chinese.

[43] J. Wu, W. Lei, Q. Wu, Y. Wang, and L. e. Ma, "Transverse vibration characteristics and stability of a moving membrane with elastic supports," *Journal of Low Frequency Noise, Vibration and Active Control*, vol. 33, no. 1, pp. 65–77, 2014.

[44] J. Wu, M. Shao, Y. Wang, Q. Wu, and Z. Nie, "Nonlinear vibration characteristics and stability of the printing moving membrane," *Journal of Low Frequency Noise, Vibration and Active Control*, vol. 36, no. 3, pp. 306–316, 2017.

[45] Y. Hu and Z. Q. Feng, "Harmonic resonance and stability analysis of axially moving rectangular plate," *Journal of Mechanical Engineering*, vol. 48, no. 09, pp. 123–128, 2012, in Chinese.

[46] Y. Z. Liu and L. Q. Chen, *Nonlinear Vibrations*, Higher Education Press, Beijing, China, 2001, in Chinese.